Journal of Applied Electrochemistry **30**: 1157–1161, 2000.

Electrocatalysis of oxygen evolution at stainless steel anodes by electrosynthesized cobalt hydroxide coatings

M. DINAMANI and P. VISHNU KAMATH*
Department of Chemistry, Central College, Bangalore University, Bangalore 560 001, India
*(*author for correspondence)*

Received 24 February 2000; accepted in revised form 21 May 2000

Key words: cobalt hydroxide, electrocatalysis, electrosynthesis, oxygen evolution

Abstract

Controlled growth of cobalt hydroxide coatings (1–2 μm thick) on stainless steel electrodes was achieved by electrogeneration of base by cathodic reduction of aqueous cobalt nitrate solutions. These coatings catalyse the oxygen evolution reaction in alkaline medium (1 M KOH) by as much as 100 mV, making cobalt hydroxide a candidate catalyst for these applications.

1. Introduction

The electrochemical evolution of oxygen from alkaline solutions is impeded by very high overpotentials. This reduces the operational efficiency of a number of electrochemical devices whose functions include the oxygen evolution reaction (OER). A number of oxide [1–5] and hydroxide [6] catalysts have been used in conjunction with nickel or stainless steel anodes to reduce the overpotential of the OER in alkaline solutions. Among these, pure [7] and doped [8, 9] nickel hydroxides have been found to be especially effective in catalysing the OER. For this application, the electrocatalyst has to be obtained in the form of a thin coating on the electrode substrate. While oxide coatings are normally prepared by pulsed laser deposition [10], r.f. sputtering [11], electron beam etching [12] or MOCVD [13], these techniques cannot be used in the case of hydroxide-electrocatalysts, as these are low temperature phases and decompose on irradiation by lasers, ion/electron beams and on heating.

Nickel hydroxide catalysts have been electrochemically prepared by electrogeneration of base, a one step method, by the cathodic reduction of an aqueous nickel nitrate solution [14, 15]. In this paper we report the controlled electrodeposition of cobalt hydroxide coatings on stainless steel electrodes. Stainless steel electrodes were chosen for this study as they are inexpensive, corrosion resistant, exhibit low oxygen evolution overpotentials and are widely employed for electrolysis of water [6].

2. Experimental details

Cobalt hydroxide was electrodeposited by the cathodic reduction of an aqueous cobalt nitrate solution (concentration, 0.1 M; pH 4.5) on a preweighed stainless steel 316 (surface area 6 cm^2) electrode in an undivided cell using a cylindrical Pt mesh (geometric area 28 cm^2) as the counter electrode. The electrodeposition was carried out galvanostatically (current densities 2–15 mA cm^{-2}) for different times (1–10 min). Within a few seconds of electrolysis, a blue coloured film of $Co(OH)_2$ began to form on the working electrode. After deposition for a fixed time, the working electrode was removed from the electrolyte, rinsed with distilled water and dried to constant weight at 65 °C. The electrode was weighed again to monitor the coating growth. Coating growth characteristics were measured as a function of deposition time, current density and electrolyte concentration. The experiments were carried out at ambient temperature (26–28 °C). The $Co(OH)_2$ coatings were uniform and adherent.

Prior to electrodeposition, the working electrode was cleaned in detergent and electrochemically polished as described elsewhere [16]. The working electrode looses 0.17 mg cm^{-2} weight during electrochemical polishing. It was observed that electrochemical polishing improves the uniformity and adherence of $Co(OH)_2$ on the stainless steel 316 substrate. On continued electrodeposition (20–25 min) the $Co(OH)_2$ coating starts flaking off and collects at the bottom of the cell. It was recovered by filtration, washed with water and dried at 65 °C. The powder sample was analyzed by powder X-ray diffractometry (Jeol JDX8P powder diffractometer), TG (lab. built system, heating rate, 5 °C min^{-1}), IR spectroscopy (Nicolet model Impact 400D FTIR spectrometer, KBr pellets, resolution 4 cm^{-1}) and scanning electron microscopy (Jeol JSM 840A scanning electron microscope).

Electrochemical measurements were performed using a Versastat model II A (EG&G PARC) scanning

potentiostat driven by model M270 electrochemistry software. Stainless steel (area 6 cm^2) flags with and without cobalt hydroxide coatings were immersed in a tank containing 1 M KOH (volume 70 ml) and polarized anodically. For elecrochemical measurements the cobalt hydroxide coatings were synthesized at a current density of 2 mA cm^{-2} for 2 min. Chronopotentiometric and chronoamperometric measurements were done for $t = 30$ min at different current densities/applied potentials. All potentials were measured with respect to a Hg/HgO (1 M KOH) electrode as reference.

In separate experiments, the coatings were found intact after prolonged electrolysis (15 h) under high pH and potential stress.

3. Results and discussion

Electrolysis of nitrate baths leads to electrogeneration of base at the cathode [17, 18] by one or more of the following reactions.
Nitrate reduction:

$$NO_3^- + 7\,H_2O + 8\,e^- \rightarrow NO_2^- + 10\,OH^- \quad (1)$$

Electrolysis of water:

$$2\,H_2O + 2\,e^- \rightarrow H_2 + 2\,OH^- \quad E^\circ = -0.828\,V \quad (2)$$

Dissolved oxygen reduction:

$$O_2 + 2\,H_2O + 4\,e^- \rightarrow 4\,OH^- \quad (3)$$

Consequently, in most nitrate baths, the metal ion is deposited as its hydroxide. In the present study, cobalt hydroxide was found to deposit as an adherent coating on the cathode. Figure 1 shows the variation of the coating weight as a function of time, current density and bath concentration. In all cases, the coating weight increases initially and then levels off. The limiting weight is much higher at low current densities (2 mA cm^{-2}) and low concentrations (0.1 M), than under other conditions. At high current densities, and high concentrations, rapid thickening and flaking of the deposit is observed. Assuming a density of 3.6 mg cm^{-3} [19] for $Co(OH)_2$, the limiting thickness of the coatings is estimated to be 1.7 to 2.3 μm. Under these conditions, the coating was found to be uniform, adherent and stable to handling and work up.

For the purpose of physical characterization the deposition was continued for up to 25 min and the flakes were collected by filtration. The powder X-ray diffraction pattern is shown in Figure 2.

Cobalt hydroxide is known to crystallize in two polymorphic modifications, known as α and β [20]. The latter, a stoichiometric compound of the composition $Co(OH)_2$ is thermodynamically the most stable phase and is isostructural with brucite, $[Mg(OH)_2]$ (Space group $P\bar{3}m1$, $a = 315$ pm; $c = 477$ pm). The α-modification is a hydroxyl deficient phase [21] with a composition $Co(OH)_{2-x}(NO_3)_x \cdot yH_2O$ ($x = 0.2$; $y = 0.67 - 1.0$) and has an increased interlayer spacing ($a = 310$ pm; $c/3 = 776$ pm). The hydroxide synthesized here is a mixed phase showing reflections characteristic

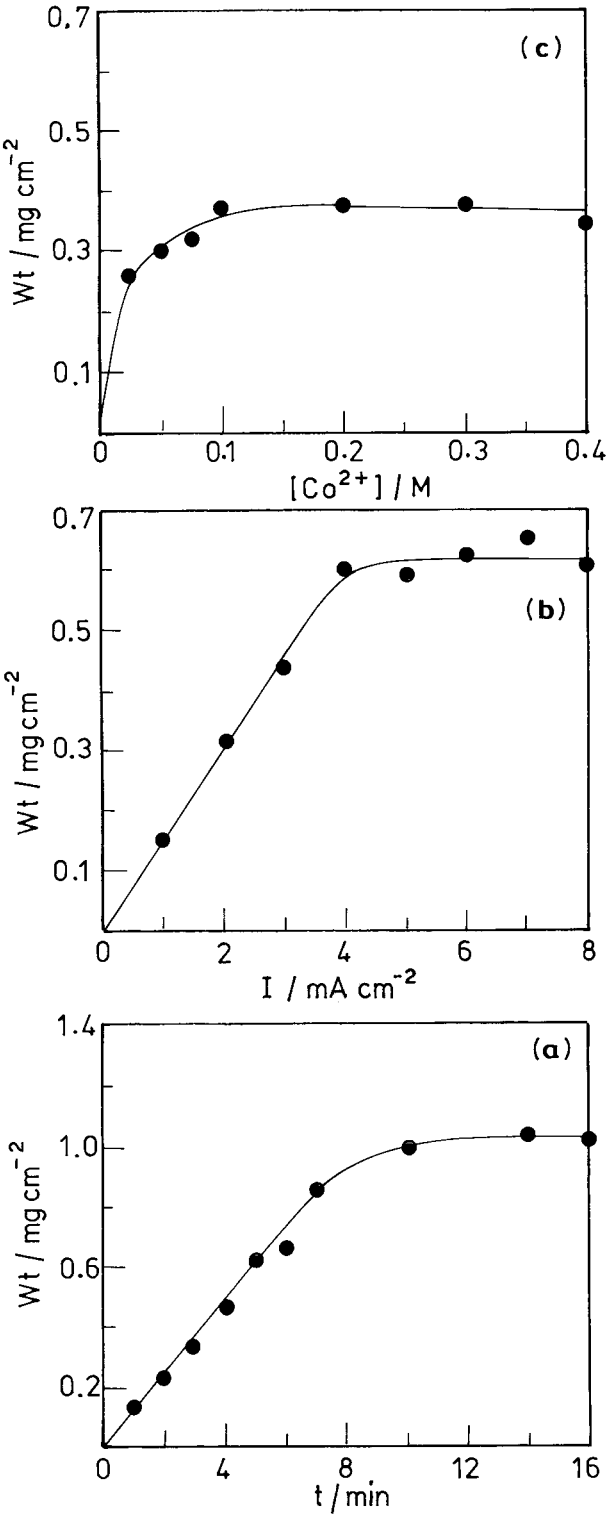

Fig. 1. Weight of the electrodeposited coating of cobalt hydroxide plotted as a function of (a) time (bath concentration 0.1 M; current 2 mA cm^{-2}), (b) current density (bath concentration 0.1 M; time 2 min) and (c) bath concentration (current density 2 mA cm^{-2}; time 2 min).

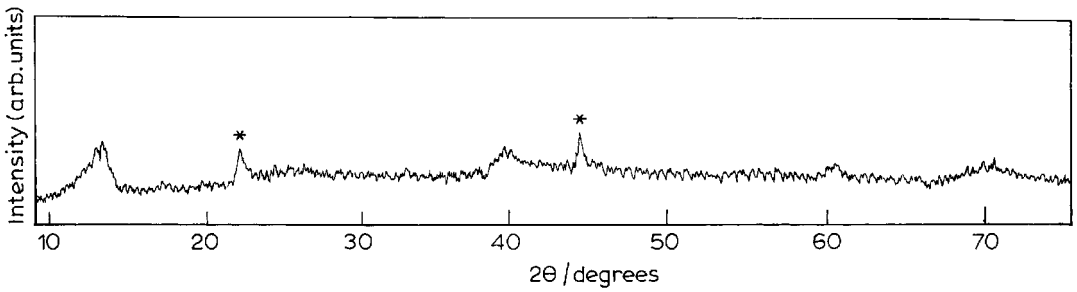

Fig. 2. Powder X-ray diffraction pattern of electrosynthesized cobalt hydroxide. Features marked by the asterisk correspond to the β modification.

of both α and β modifications. The low angle peak at 778 pm is characteristic of the (0 0 3) reflection of the α-phase while the peaks at 465 pm and 237 pm are characteristic of the (0 0 1) and (1 0 1) reflections of the β-phase. The broad 'saw-tooth' band at 268 pm is due to the two-dimensional (1 0) reflection of the turbostratically disordered α-cobalt hydroxide [21].

The α-modification is metastable and ages rapidly to the β-form under the conditions adopted for the OER. Therefore no attempts were made to synthesize single-phase hydroxide coatings. The infrared spectrum also shows vibrations characteristic of the α (hydrogen bonded OH stretch, 3457 cm^{-1}; vibrations due to intercalated nitrate, 1465, 1387, 839 cm^{-1}; hydrogen bonded Co—O—H bending vibration, 640 cm^{-1}) and the β (nonhydrogen bonded OH stretch, 3640 cm^{-1} and Co—O—H bending vibration, 513 cm^{-1}) phases. The TG data show that the material undergoes a single step weight loss of 26% which is intermediate between that expected for the α (29.6%) and β (13.4%) modifications [20].

Figure 3 shows the cyclic voltammograms for the bare stainless steel and cobalt hydroxide covered stainless steel electrodes. It is evident that oxygen evolution is initiated at a much lower potential (580 mV) on the cobalt hydroxide covered electrode compared to the bare stainless steel electrode (670 mV). The strong anodic peak seen in the former corresponds to the oxidation of cobalt hydroxide [22].

For a more detailed study, the oxygen evolution currents were measured for different applied potentials (chronoamperometry) and the oxygen evolution potentials measured for different currents (chronopotentiometry). Typical measurements are shown in Figure 4. The measured values of the current (potential) for different applied potentials (currents) are plotted in Figure 5. It is clear that over a range of applied potentials and currents, the cobalt hydroxide coated electrode catalyses the OER. The catalysis is by as much as 100 mV in galvanostatic experiments and by a twofold increase in current in potentiostatic experiments. This compares favourably with the performance of nickel hydroxide coated electrodes [7].

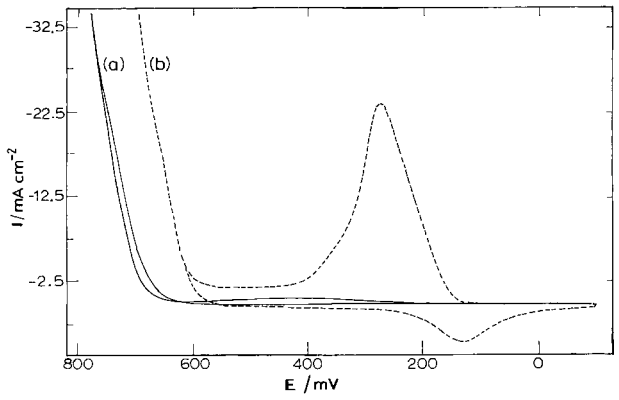

Fig. 3. Cyclic voltammograms of (a) bare stainless steel and (b) cobalt hydroxide covered stainless steel electrodes (scan rate 20 mV s^{-1}; initial potential −100 mV; vertex potential 800 mV).

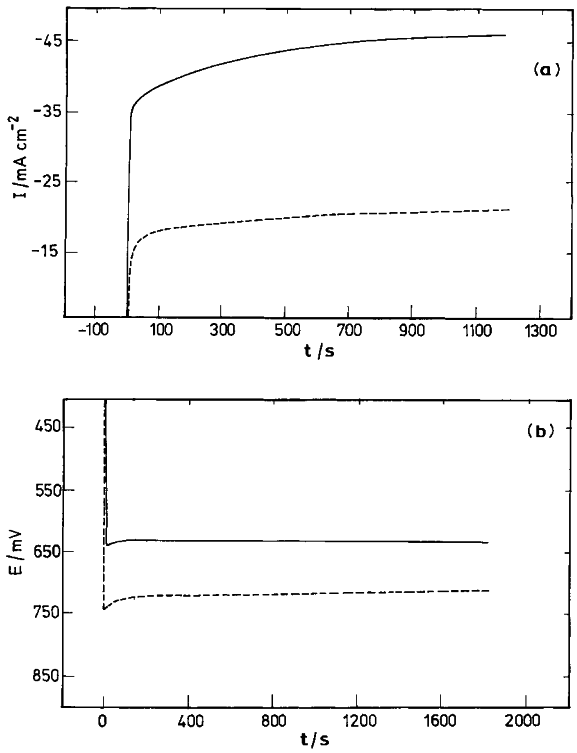

Fig. 4. (a) A typical chronoamperogram (660 mV) and (b) a typical chronopotentiogram (50 mA cm^{-2}) recorded for the OER at a bare (dotted line) and a cobalt hydroxide covered (full line) stainless steel electrode.

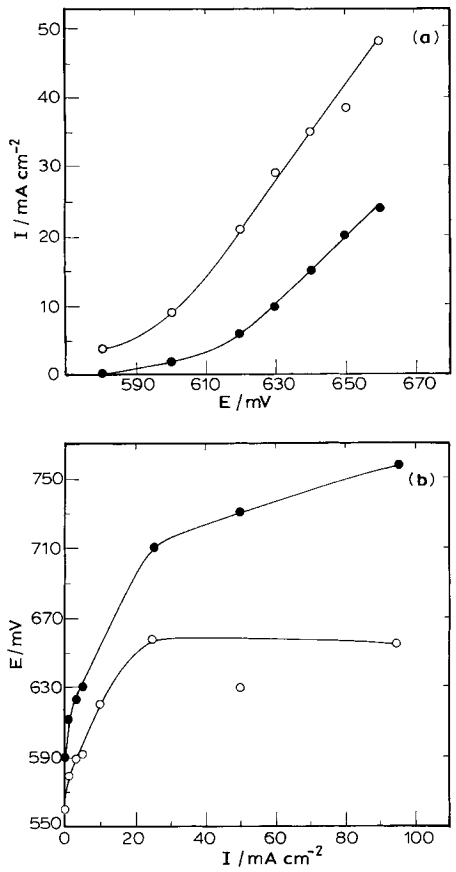

◀

Fig. 5. (a) Measured values of oxygen evolution currents at different applied potentials. (b) Measured values of oxygen evolution potentials at different applied currents (closed circles, bare stainless steel; open circles, cobalt hydroxide covered stainless steel).

As in the case of nickel hydroxide, oxygen evolution is catalysed through the formation of the higher valent hydroxide of Co [22]. This is indicated by the chronopotentiogram recorded at low current (Figure 6). A clear plateau is seen after 900 s when the potential

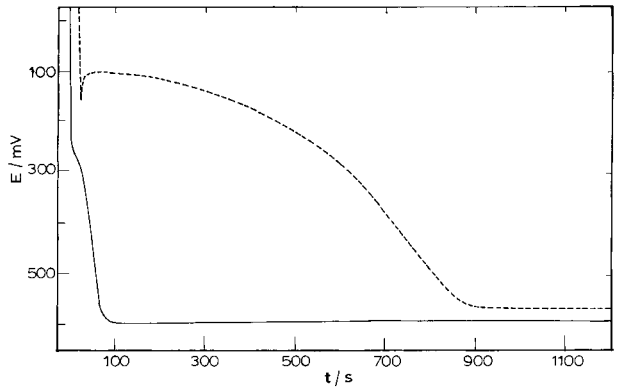

Fig. 6. Chronopotentiogram recorded at 0.16 mA cm^{-2} for the bare (full line) and cobalt hydroxide covered (dotted line) stainless steel electrode.

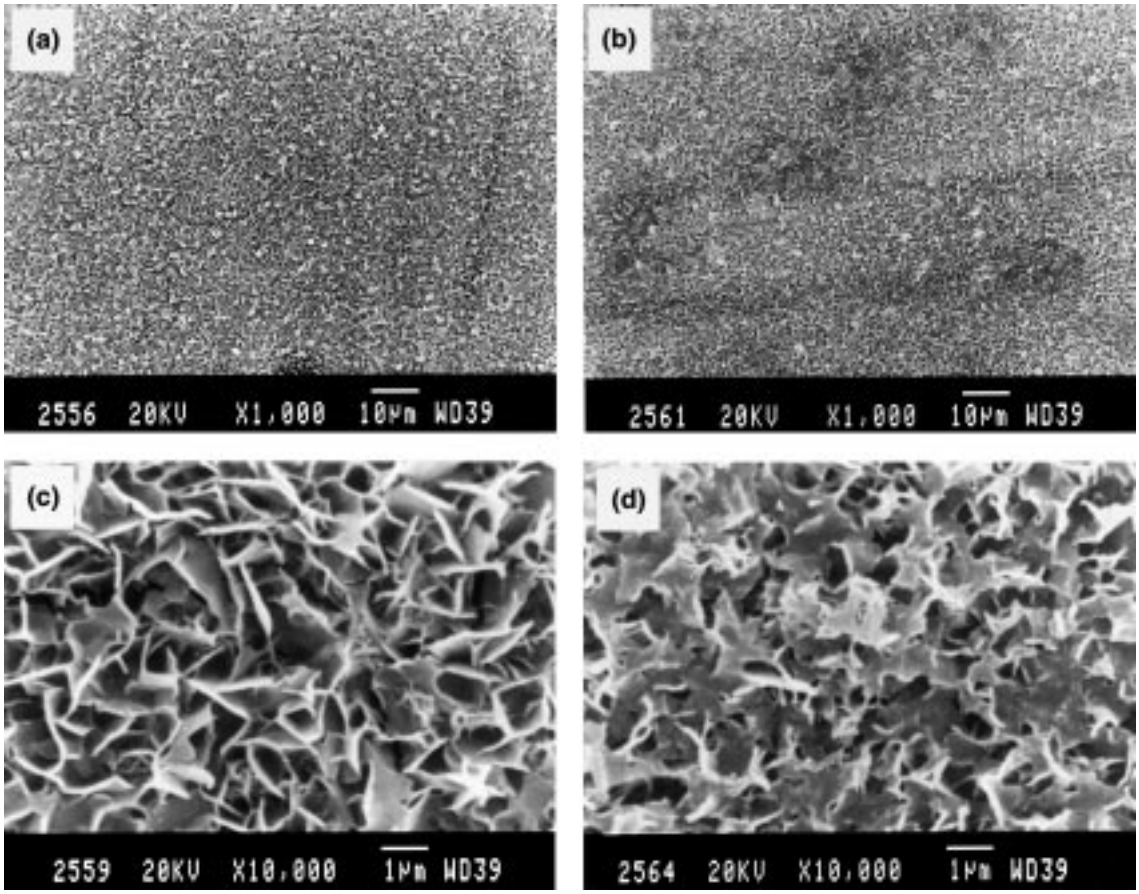

Fig. 7. Scanning electron micrographs of the cobalt hydroxide covered stainless steel electrode before (a, c) and after (b, d) oxidation.

corresponding to the OER is attained. The initial variation in potential corresponds to the oxidation of $Co(OH)_2$. The charge consumed by cobalt hydroxide as estimated from the chronopotentiogram amounts to the oxidation of Co from the +2 state to the +2.4 or 2.5 state depending on whether the hydroxide is of the β (molecular weight 92.8) or the α (molecular weight, 116) variety. The oxidation reaction can be approximately shown as

$$Co(OH)_2 + OH^- \rightarrow CoO(OH) + H_2O + e^-$$

When the cobalt hydroxide is completely oxidized, the excess oxygen is evolved.

Figure 7 shows the scanning electron micrographs of the as-prepared and oxidized coatings. The low magnification micrographs clearly show that the coverage of the substrate is uniform. Under high magnification, a porous funnel shaped morphology comprising scales growing perpendicular to the substrate can be seen in the as-prepared coating. The porous morphology is ideally suited for electrocatalysis. After oxygen evolution, there is no change in the nature of the coating under low magnification, but under high magnification, the edges of the funnels appear broken.

In conclusion, we have demonstrated the controlled growth of cobalt hydroxide coatings on stainless steel substrates by electrogeneration of base. The coatings are good catalysts for oxygen evolution in alkaline medium.

Acknowledgements

The authors thank the Department of Science and Technology for financial support, the Solid State and Structural Chemistry Unit and the Department of Metallurgy, Indian Institute of Science for powder X-ray diffraction and electron microscopy facilities respectively.

References

1. I. Nikolov, R. Darkaoui, E. Zhecheva, R. Stoyanova, N. Dimitrov and T. Vitanov, *J. Electroanal. Chem.* **362** (1993) 119.
2. A.C.C. Tseung and S. Jasem, *Electrochim. Acta* **22** (1977) 31.
3. M.R. Gennero de Chialvo and A.C. Chialvo, *Electrochim. Acta* **38** (1993) 2247.
4. M. El Baydi, G. Poillerat, J.-L. Rehspringer, J.L. Guatier, J.-F. Koenig and P. Chartier, *J. Solid State Chem.* **109** (1994) 281.
5. R.N. Singh, L. Bahadur, J.P. Pandey and S.P. Singh, *J. Appl. Electrochem.* **24** (1994) 149.
6. S.K. Tiwari, A.K.L. Singh and R.N. Singh, *J. Electroanal. Chem.* **319** (1991) 263.
7. D.E. Hall, *J. Electrochem. Soc.* **130** (1983) 317.
8. D.A. Corrigan and R.M. Bendert, *J. Electrochem. Soc.* **136** (1983) 723.
9. S.I. Cardoba, R.E. Carbonio, M.L. Teijelo and V.A. Macagno, *Electrochim. Acta* **31** (1986) 1321.
10. H. Yugami, H. Naito, H. Arashi and M. Ishigame, *Solid State Ionics* **86** (1996) 1307.
11. B.Y. Liaw, R.E. Rocheleau and Q.H. Gao, *Solid State Ionics* **92** (1996) 85.
12. C. Byun, J.W. Jang, I.T. Kim, K.S. Hong and B.W. Lee, *Mat. Res. Bull.* **32** (1997) 431.
13. M. Hartamanova, I. Thurzo, M. Jergl, J. Bartos, F. Kadlec, V. Zelenzy, D. Tunega, F. Kundracik, S. Chromic and M. Brunel, *J. Mater. Sci.* **33** (1998) 969.
14. I.G. Casella, M.R. Guascito and M.G. Sannazzaro, *J. Electroanal. Chem.* **462** (1999) 202.
15. I.G. Casella and M.R. Guascito, *Electrochim. Acta* **45** (1999) 1113.
16. D.A. Corrigan, *J. Electrochem. Soc.* **134** (1987) 377.
17. J.A. Switzer, *Am. Ceram. Soc. Bull.* **66** (1987) 1521.
18. Y. Matsumoto, T. Morikawa, H. Adachi and J. Hombo, *Mater. Res. Bull.* **27** (1992) 1319.
19. R.C. Weast (ed.), 'The Handbook of Chemistry and Physics', (Chemical Rubber Co., Cleveland, 1986).
20. J. Ismail, M.F. Ahmed, P.V. Kamath, G.N. Subbanna, S. Uma and J. Gopalakrishnan, *J. Solid State Chem.* **114** (1995) 550.
21. R.S. Jayashree and P.V. Kamath, *J. Mater. Chem.* **9** (1999) 961.
22. J. Ismail, M.F. Ahmed and P.V. Kamath, *J. Power Sources* **36** (1991) 507.